FATIGUE FRACTURE MECHANISM OF ZIRCONIA SHOT PEENED Ti–6Al–4V ALLOY

Kiyotaka MASAKI[a], Noriyuki HISAMORI[b], Yuji KOBAYASHI[c], and Daisuke GOWA[c]

[a] Okinawa College, National Institute of Technology, JAPAN, masaki-k@okinawa-ct.ac.jp
[b] Sophia University, JAPAN, hisamori@me.sophia.ac.jp;
[c] SINTOKOGIO Ltd, JAPAN, y-kobayashi@sinto.co.jp, d-gowa@sinto.co.jp

Keywords: Shot peening, Ti–6Al–4V, High cycle fatigue, Fracture mechanism, Tensile axial loading

Introduction

Ti–6Al–4V is the most popular titanium alloy. It is used for aerospace industrial components and biomedical materials because of its high tensile strength at high temperatures and high corrosion resistance. In many cases, industrial components are subjected to cyclic loadings when they are used. Therefore, improvement in high cycle fatigue properties is essential to enhance the reliability of the components. We have been attempting to improve the high cycle fatigue properties by zirconia shot peening treatment of Ti–6Al–4V. At the 12th International Conference on Shot Peening, we reported that zirconia shot peening could extend the rotating bending fatigue life of Ti–6Al–4V, but could not improve the fatigue strength for a high cycle regime. We indicated that changes in the fatigue property resulted from the residual stresses that arose from the treatment. In this study, the effects of the shot peening treatment on pulsating tensile axial loading fatigue and its fracture mechanism were investigated.

Objectives

Ti-6Al-4V is the most popular titanium alloy used for aerospace industrial components [1,2] and biomedical materials [3-5] because it has high corrosion and high tensile strength at high temperatures. In many cases, the cyclic load acts on the components while they are used; therefore, it is necessary to improve the high cycle fatigue property to enhance the reliability of components. We have earlier reported that zirconia shot peening could extend the rotating bending fatigue life of Ti–6Al–4V, but could not improve the fatigue strength for a high cycle regime [6]. Then, we reported that the cause of fatigue failure of the shot peened specimen under the fatigue limit of the non peened specimen was the fatigue crack initiated from an α-Ti facet at the subsurface, as shown in Fig. 1. In this report, pulsating tensile axial loading fatigue tests using the shot peened specimen with same zirconia shot peening conditions were conducted in order to further investigate the relation between facet generation and fatigue fracture.

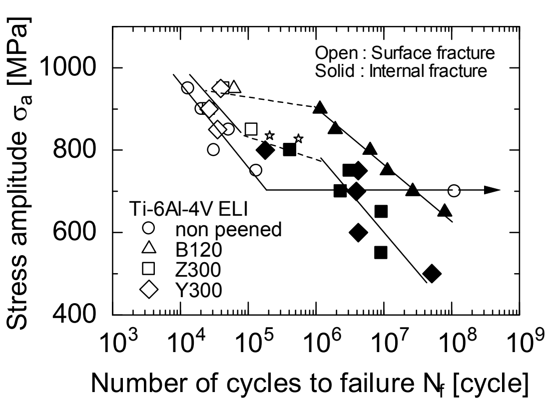

(a)S-N diagram

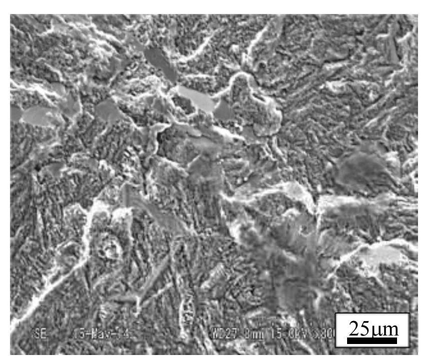

(b) Crack initiation site of fish eye.
(4mm, Y300, 600MPa, 4.19×10^6cycle)

Fig.1 Rotating bending fatigue results [6].

Methodology

Material and Fatigue Specimens: The material used in this study is Ti-6Al-4V titanium alloy prepared through hot working. Before machining, the solution was heated, followed by water cooling after being heated at 960 °C for 60 min, and air cooling after being heated at 550 °C for 360 min. Table 1 shows the chemical compositions and Table 2 shows the mechanical properties of the material. Fig. 2 exhibits the microstructure of the cross and longitudinal sections of the material. The material has a bimodal microstructure in which the fine grains of the α-Ti matrix are homogeneously dispersed in the lamellar structure of an α+β-Ti structure. The size of the α-Ti matrix is about 10 μm. Fig. 3 shows the shape of the fatigue test specimens, which is a simple hour-glass type with a shallow notch of 3 or 4 mm in diameter. The central part of the specimen was designed in the same shape as the rotary bending fatigue test specimen [6]. The stress concentration factors were 1.07 for the 3 mm specimen and 1.10 for the 4 mm specimen [7]. After machining, the surface of the shallow notch was mirror finished by emery paper and buff cloth with alumina liquid of 1 μm and 0.1 μm.

Table 1 Chemical composition [wt%]

Ti	Al	V	O	Fe	C	N	H
Bal	6.14	4.06	0.17	0.15	0.01	<0.01	0.01

Table 2 Mechanical properties.

Tensile strength [MPa]	Yield stress [MPa]	Elongation [%]
1178	1107	8.4

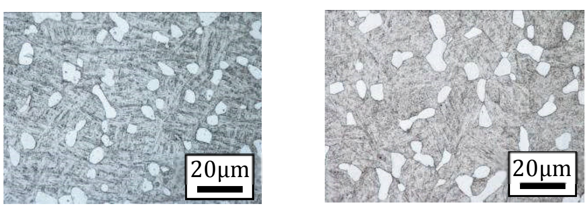

(a) Cross section (b) Longitudinal section

Fig.2 Microstructure of material.

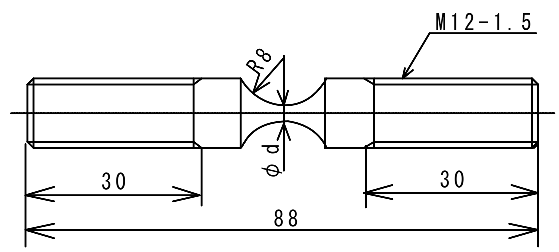

Fig.3 Configuration of fatigue specimens, mm.

Shot Peening Conditions: Shot peening was conducted with three types of fine zirconia shot grids. Fig. 4 shows a macro photograph of the shot grids. The average diameter of the B120 grids was about 0.12 mm and those of Z300 and Y300 grids were 0.3 mm. The difference between the Z300 and Y300 grids is the material grades. The grade of the Y300 is higher than that of the Z300. Table 3 shows the shot peening conditions. All shot peening treatments were conducted under mild conditions using an air-type shot peening machine. The air pressure of all treatments was 0.5 MPa. The Almen intensities of the treatments were between 0.2 and 0.35 mmN.

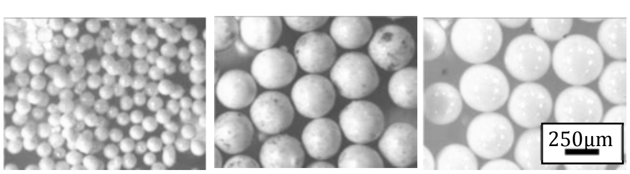

(a) B120 (b) Z300 (c) Y300

Fig.4 Shot grids.

Table 3 Conditions of shot peening.

Shot material	B120	Z300	Y300
Shot diameter [mm]	0.12	0.3	0.3
Peening time [s]	24	24	32
Air Pressure [MPa]	0.5		
Arc Height [mmN]	0.205	0.31	0.352
Cover rage [%]	over 100		

Fatigue Tests and Fracture Surface Observation: High-cycle fatigue tests were conducted with a hydraulic servo-type axial fatigue testing machine in air at room temperature. The stress ratio was R = 0.1 and the frequency of the fatigue loading was 10 Hz. After the fatigue fracture of the specimens, all of the fracture surfaces were observed by a stereoscopic microscope and a scanning electron microscope (SEM) in order to investigate the fatigue crack initiation site.

Results and Analysis

Peening Effects: The peening effect generated in the axial loading fatigue test specimen used in this study is considered equivalent to the rotary bending fatigue test specimen that we used in our earlier work, because the shape and size of the central part of the test specimen are the same [6].
Table 4 shows the surface roughness of all specimens, which increases with shot peening. Here, Ra is the average roughness, Ry is the maximum height, and Rz is the 10-point average roughness over the length of 4 mm. Rz of the B120, Z300, and Y300 grids after shot peening were about 7.6, 7.4, and 10.8 times greater compared with that of the non peened materials.
Fig. 5 shows the hardness distribution of all the specimens from the surface to a depth of 0.1 mm. The hardness of the Ti-6Al-4V matrix was about 370 HV. The surface hardening of the non peened specimen was about 450 HV. The hardness may be affected by machine processing when making the specimens. The surface hardness values of the Z300, Y300, and B120 grids were 495 HV, 510 HV, and 460 HV, respectively.
Fig. 6 shows the residual stress distributions. The residual stress was measured by X-ray diffraction (XRD) with Cu-Kα radiation (50 kV, 30 mA) applying the sin2ψ-method on the {213}-plane of the hexagonal α-phase Ti and K = -217 MPa/deg as a stress constant [8]. In all of the specimens, compressive residual stress exists on the surface. The largest compressive residual stress was about 1150 MPa on the B120. The Z300 and Y300 grids have similar the residual stress distribution profiles, with the compressive residual stress of about 750 MPa on the surface. Each zero crossing point of the residual stress distribution in the specimen was about 20 μm for the non peened material, about 40 μm for the B120 specimen, and about 100 μm for the Z300 and Y300 specimens.

Table 4 Surface roughness values [μm]

	3mm			4mm		
	R_a	R_z	R_{zjis}	R_a	R_z	R_{zjis}
n.p.	0.15	1.1	0.8	0.15	0.8	0.5
B120	0.96	6.5	4.6	0.72	5.2	3.8
Z300	1.08	6.7	4.4	0.88	6.1	3.7
Y300	2.12	10.5	7.2	1.43	7.7	5.4

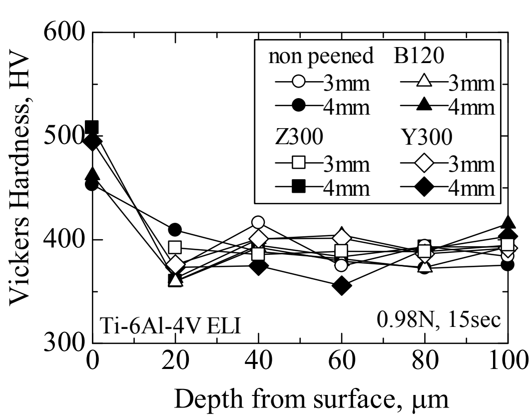

Fig.5 Vickers hardness distributions.

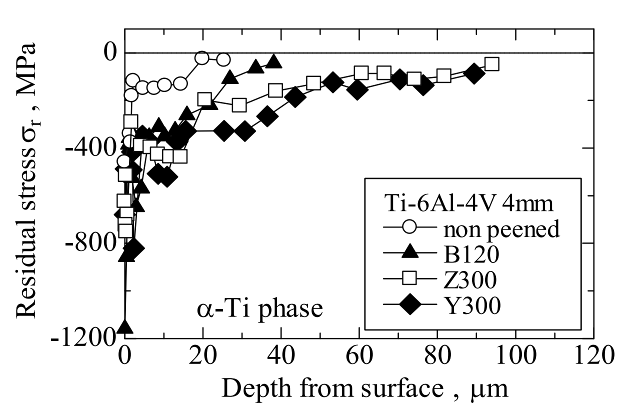

Fig.6 Residual stress distributions.

Fatigue Results: Fig. 7 shows the S-N diagram of the fatigue testing results of all materials. The vertical axis shows the maximum stress considering the stress concentration. All experimental data can be approximated by one straight line, regardless of the shot peening conditions. In the shot peening treatment conditions used in this study, no fatigue property improvement was observed. The fatigue strength at 10^7 cycles of the non peened specimen was about 500 MPa, which was 200 MPa lower than the value of the rotating bending loading, as shown in Fig. 1. The value of 500 MPa is roughly the same as the tensile strength of pure titanium with an α-Ti matrix. The fatigue limits of the shot peened specimens are expected to be even lower. The white symbols in Fig. 7 represent the fracture from the surface of the specimen, while the solid symbols represent the fracture from inside the specimen. Many of the specimens were fractured from inside the specimen. Examples of the fracture surface from inside the specimen were observed by SEM and are shown in Fig. 8. There are many facets of the α-Ti matrix visible at the crack initiation site on the fracture surface.

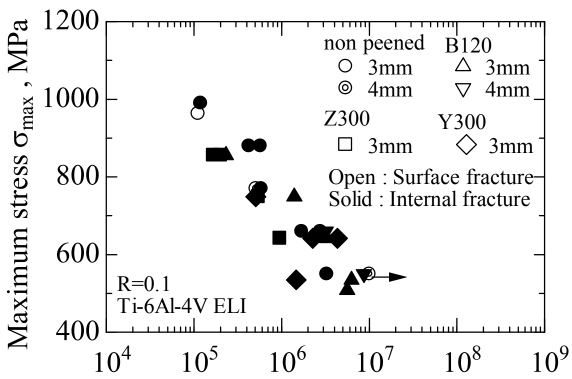

Fig.7 S-N diagram of axial loading fatigue results.

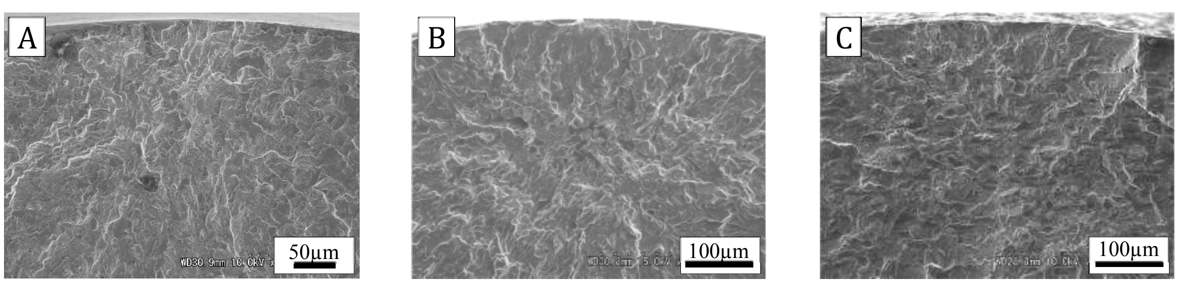

(a) Low magnification image.

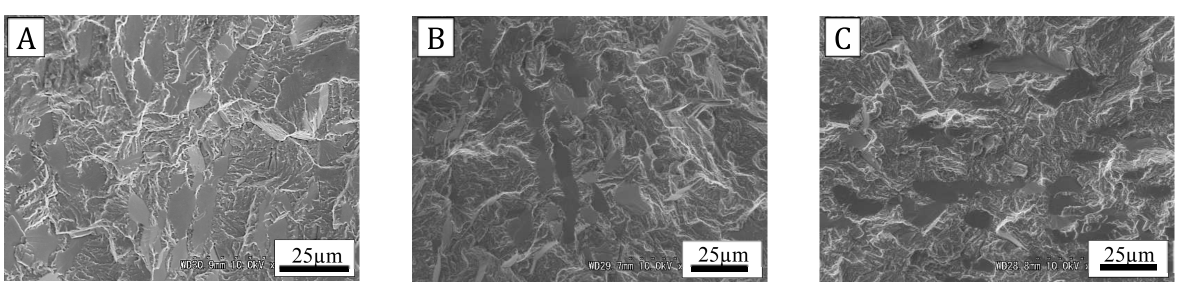

(b) High magnification image.

Fig.8 Fracture surface of the axial load fatigue test. (A) 3mm non peened (749 MPa, 5.83×10^5 cycle), (B) 3mm Y300 (642 MPa, 4.32×10^6 cycle), (C)3mm B120 (535 MPa, 6.26×10^6 cycle)

α-Ti Facet Generation and Fatigue Fracture: The α-Ti facet was observed in all the fatigue fracture surfaces under the pulsating tensile axial loading conditions. However, in the rotating bending loading fatigue test in which the tensile stress and compressive stress act alternately, even when the stress amplitude exceeds 700 MPa, the α-Ti facet was not observed at the crack initiation site on the fatigue fracture surface of the non peened specimen. Also, fatigue failure did not occur at 700 MPa or less on the non peened specimen [6]. In other words, the α-Ti facet is generated when a tensile stress of 500 MPa is applied without compressive stress. On the other hand, it is considered that compressive stress exerts some influence on the fatigue fracture of the shot peened specimen because high compressive residual stress acts near the specimen surface, as shown in Fig. 6. Fig. 9 shows the depth from the specimen surface of the crack initiation site on the fatigue fracture surface. The depth of the crack initiation site of the shot peened specimen was deeper than that of the non peened specimen, and all of them were located 100 μm or more from the surface. This depth is deeper than that of the zero crossing point of the residual stress distribution, as shown in Fig. 6. That is, the crack initiation site is located at a position where the compressive stress does not act or where the tensile residual stress acts to balance the residual compressive stress. As a result, the α-Ti facet is generated easily and a fatigue crack propagates smoothly. If the fatigue crack initiates at the position where the tensile residual stress is generated, the fatigue limit of the shot peened specimen will be lower than that of the non peened specimen.

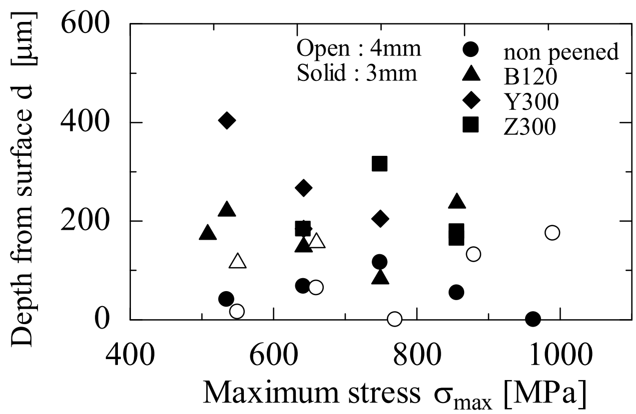

Fig.9 Depth of crack initiation sites.

Conclusions

Pulsating tensile axial loading fatigue testing of the Ti-6Al-4V material was performed to investigate the effects of shot peening with three types of fine zirconia shot, namely B120, Z300, and Y300. The results are summarized as follows:

(1) The fatigue strength at 10^7 cycles of the non peened specimen under pulsating tensile axial loading conditions is about 500 MPa, which is the same as the tensile strength of the pure Ti material that constructed the α-Ti matrix. This value is 200 MPa lower than that observed under the rotating bending loading conditions.
(2) The fatigue life of the non peened specimen cannot be extended and the fatigue limit cannot be improved by fine zirconia shot peening under the conditions employed in this study. Moreover, the fatigue strength at 10^7 cycles was reduced by shot peening.
(3) Almost all of the specimens are fractured from the α-Ti facet inside the specimen. It is expected that the α-Ti facet is generated when a tensile stress of 500 MPa is applied without compressive stress.
(4) The depth of the crack initiation site of the shot peened specimen was deeper than that of the non peened specimen, and all of them were located at 100 μm or more from the surface. This depth is deeper than the depth of the zero crossing point of the residual stress distribution.

Because the crack initiation site is located at the position where the tensile residual stress acts to balance the residual compressive stress, the fatigue strength at 10^7 cycles of the shot peened specimen is lower than that of the non peened specimen.

References

[1] R.R. Boyer, An overview on the use of titanium in the aerospace industry, Materials Science and Engineering Vol.A213 (1996) pp.103-114.
[2] R.O. Ritchie, B.L. Boyce, J.P. Campbell, O. Roder, A.W. Thompson and W.W. Milligan, Thresholds for high-cycle fatigue in a turbine engine Ti–6Al–4V alloy, International Journal of Fatigue Vol.21 (1999) pp.653–662.
[3] L.R. Saitova, H.W. Höppel, M. Göken, I.P. Semenova and R.Z. Valiev, Cyclic deformation behavior and fatigue lives of ultrafine-grained Ti-6AL-4V ELI alloy for medical use, International Journal of Fatigue Vol.31 (2009) pp.322–331.
[4] B. Hamilton, S. Oppenheimer, D. C. Dunand and D. Lewis, Diffusion Bonding of Ti-6Al-4V Sheet with Ti-6Al-4V Foam for Biomedical Implant Applications, Metallurgical and Materials Transactions B, Vol.44 (2013) pp.1554–1559.
[5] T. Hanaka, Biocompatibility of titanium - favorable properties, Journal of The Japan Institute of Light Metals, Vol.62 (2012） pp.285–290.
[6]K. Masaki, N. Hisamori, Y. Kobayashi and D. Gowa, effects of zirconia shot peening on high cycle fatigue properties of TI-6Al-4V alloy, Proc. of The 12th ICSP, (2014) pp.90-95.
[7] W. D. Pilkey, D. F. Pilkey, Peterson's Stress Concentration Factors, John Wiley & Sons, inc. (2007)
[8] N. Tsuji, S. Tanaka and T. Takasugi, Effects of combined plasma-carburizing and shot-peening on fatigue and wear properties of Ti–6Al–4V alloy, Surface & Coatings Technology Vol.203 (2009) pp.1400–1405.